Magnetic Resonance Materials in Physics, Biology and Medicine (2020) 33:367–376
https://doi.org/10.1007/s10334-019-00785-9

RESEARCH ARTICLE

Intravascular signal suppression and microvascular signal mapping using delays alternating with nutation for tailored excitation (DANTE) pulse for arterial spin labeling perfusion imaging

Yasuhiro Fujiwara[1] · Hirohiko Kimura[2] · Shota Ishida[3] · Masayuki Kanamoto[3] · Naoyuki Takei[4] · Tsuyoshi Matsuda[5] · Nobuyuki Kosaka[2] · Toshiki Adachi[3]

Received: 17 April 2019 / Revised: 30 September 2019 / Accepted: 5 October 2019 / Published online: 17 October 2019

Abstract

Objective To optimize the delays alternating with nutation for tailored excitation (DANTE) pulse as a vascular crushing gradient to eliminate macro-and micro-vascular signals and to generate a macrovascular space-related map by applying DANTE with multiple conditions.

Materials and methods Numerical simulation was performed to estimate the optimal flip angle (FA) of the DANTE. A phantom study was conducted to evaluate the impact of the FA and gradient area (GA) of the DANTE with three flow velocities and various parameters of the DANTE. Finally, an in vivo study was performed to assess the optimal DANTE parameters and to map the estimated macrovascular signal of the arterial spin labeling (ASL) signal.

Results Numerical simulation revealed that the decrease of magnetization plateaued at 12.5° of FA. The phantom study showed that the setting of larger FA or GA decreased the ASL signals. The decrease of the ASL signal depended on the flow velocity, and the dependence increased with decreasing GA. The in vivo study revealed that larger FA and GA decreased the perfusion signal.

Discussion An optimized DANTE makes it possible to efficiently suppress the macro-and-micro vascular signals depending on the flow velocity. Moreover, macrovascular signal mapping may be useful to assess altered hemodynamic states.

Keywords Magnetic resonance imaging (MRI) · Arterial spin labeling (ASL) · Perfusion · Cerebral blood flow (CBF) · Quantification

Introduction

Arterial spin labeling (ASL) is a noninvasive method for evaluating brain perfusion, which allows quantitative measurement of the regional cerebral blood flow (rCBF) [1–3]. ASL has been widely used in magnetic resonance imaging (MRI) examination for various brain diseases, such as cerebrovascular disease and brain tumors [4–6].

In ASL perfusion imaging, it is well known that the signal from the label remains in larger arteries at the time of imaging causing a vascular artifact as a high signal intensity [7–10]. This artifact reduces the accuracy of quantification of the arterial transit time (ATT) and rCBF when the ATT is longer than the post-labeling delay time [11]. Therefore, it is necessary to clarify the differences between the ASL signals originating from a large vessel and those originating from the microvasculature, for measuring the rCBF accurately [11].

✉ Hirohiko Kimura
kimura@u-fukui.ac.jp

1 Department of Medical Image Sciences, Faculty of Life Sciences, Kumamoto University, Kumamoto, Japan

2 Department of Radiology, Faculty of Medical Sciences, University of Fukui, 23 Shimozaizuki, Eiheiji-Matsuoka, Yoshida-gun, Fukui 910-1193, Japan

3 Radiological Center, University of Fukui Hospital, Fukui, Japan

4 Global MR Applications and Workflow, GE Healthcare Japan Corporation, Tokyo, Japan

5 Division of Ultra-high Field MRI, Institute for Biomedical Science, Iwate Medical University, Iwate, Japan

The use of vascular crusher gradients after labeling pulse or motion-sensitized T_2-preparation module has been reported as a signal suppression method due to spin remaining in the larger arteries [12]. Recently, Matsuda et al. reported that the vascular signal is more uniformly reduced with the use of the delays alternating with nutation for tailored excitation (DANTE) preparation pulse than with motion-sensitized driven-equilibrium [13]. However, the optimal conditions for applying DANTE to ASL perfusion imaging have not been investigated. Theoretically, it has been reported that the DANTE can change the degree of suppression of vascular signal by changing the flip angle (FA) [14]. In addition, the vascular signal can be suppressed not only by the use of the FA but also the strength of the gradient pulse. Therefore, it is necessary to optimize DANTE by adjusting these parameters to suppress vascular signals in ASL imaging effectively.

In addition, we hypothesized that applying DANTE to the labeled spins could suppress not only macrovascular but also microvascular signals. The flow velocity of labeled spins should dynamically vary from macrovasculature to extravasculature. It was reported that the average blood flow velocity of the basal ganglia and semiovale center were 4.6 cm/s and 0.63 cm/s, respectively [15]. The flow velocity of the capillary bed was reported as 0.2–5.0 mm/s [16]. When the macro-and micro-vascular signals in labeled spins are eliminated using DANTE with flow velocity dependence, the extravascular signal can be discriminated. Theoretically, the rCBF measured based on the extravascular-spin-dominated signal should be close to the rCBF measured using positron emission tomography rather than the rCBF measured by ASL signal from all labeled spins, since rCBF measurement in PET is performed with extravascular distribution of the tracer [17].

Moreover, we hypothesized that the macrovascular signal-related map can be generated using multiple ASL images with DANTE at multiple suppression conditions depending on flow velocity. Macrovascular signal mapping may be useful to obtain information regarding regional macrovascular signals, which likely decreases during a compromised perfusion state due to up-stream vascular stenosis.

The purpose of this study was to optimize the flow crushing gradient used in the DANTE module for efficiently eliminating macro-and micro-vascular signals and to generate a macrovascular signal-related map using ASL images with DANTE.

Materials and methods

All images were obtained on a 3.0 T MRI (Discovery MR750; GE Healthcare, Milwaukee, WI, USA) with a 32-channel phased-array head coil. The study protocol was approved by the institutional review board of the University of Fukui.

The ASL sequence and DANTE preparation module are shown in Fig. 1. The radio frequency (RF) pulse train of the DANTE was a rapid series of low FAs with nonselective RF pulses and gradient pulses [14]. The DANTE was applied between the last two background suppression pulses of the ASL sequence [13]. The FA of the DANTE changed its polarity alternatively. The gradient of the DANTE was applied in the static magnetic field direction along with the direction of the blood vessel in the brain. Moreover, the

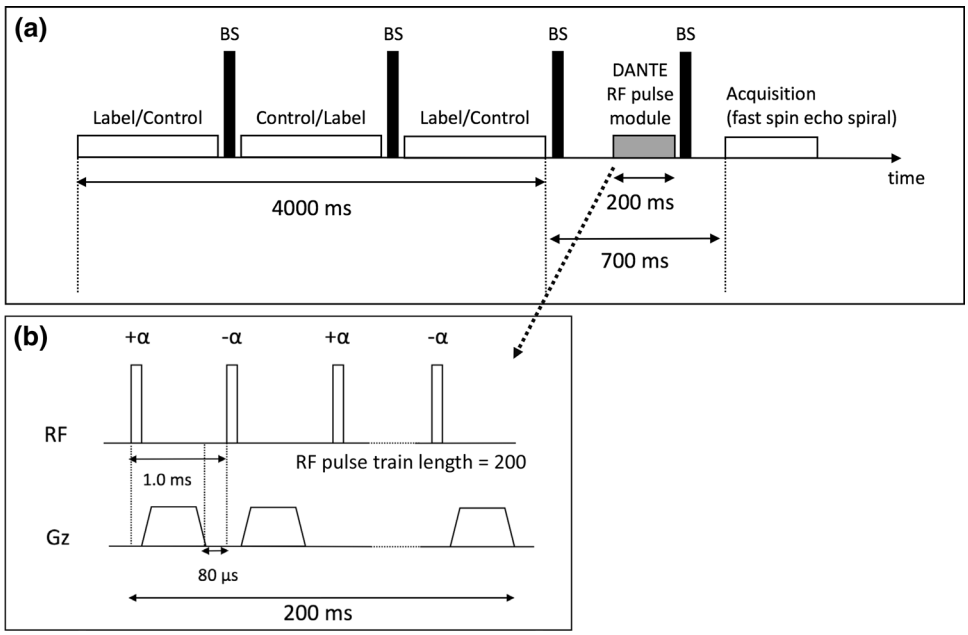

Fig. 1 Schematic diagram of the arterial spin labeling sequence (**a**) and the delays alternating with nutation for tailored excitation (DANTE) pulse module (**b**). The DANTE module was inserted between the last two background suppression pulses (BS)

gradient of the DANTE was adjusted by the gradient area (GA) defined by multiplying gradient strength and duration. The applied parameters of the DANTE were as follows: RF pulse duration, 100 μs; dead time from the end of the gradient pulse to the DANTE, 80 μs; the time interval between successive RF pulses, 1.0 ms; and the number of the DANTE RF pulses, 200. In this study, all perfusion images were acquired using pseudo-continuous labeling with three-dimensional (3D) fast spin-echo with a spiral acquisition.

Numerical simulation

To estimate the optimal FA of the DANTE, static and flowing magnetization after applying the DANTE were simulated using the equations reported by Li et al. [14], considering the following parameters: T_1 value of static tissue, 1200 ms; T_1 value of blood, 1600 ms; the time interval between successive RF pulses, 1.0 ms; the number of DANTE, 200; and FAs of DANTE, 0°–30°.

The longitudinal magnetization for static spin ($M_{n,z}$) was estimated from the following equation:

$$M_{n,z} = E_{1,\mathrm{app}}^{n}\left(M_{\mathrm{ini},z} - M_{\mathrm{pss},z}\right) + M_{\mathrm{pss},z}, \tag{1}$$

where $M_{\mathrm{ini},z}$ and $M_{\mathrm{pss},z}$ are the initial and pseudo-steady state longitudinal magnetization for static spin, n is the number of DANTE. $E_{1,\mathrm{app}}$ is the an apparent T_1 decay over two periods of DANTE pulses for tissue ($E_{1,\mathrm{app}}$), which is estimated from the following equations:

$$E_1 = \mathrm{e}^{\left(-TR/T_{1,\mathrm{tissue}}\right)}, \tag{2}$$

$$E_{1,\mathrm{app}} = \sqrt{E_1^2 \cos^2\alpha - E_1 \cos\theta \sin^2\alpha}, \tag{3}$$

where θ shows the generalized precession angle, which is the phase angle between the nth RF pulse and the magnetization immediately before this pulse. α is the FA of the DANTE pulse. Finally, the longitudinal magnetization for static spin ($M_{\mathrm{pss},z}$) was calculated using the following equation:

$$M_{\mathrm{pss},z} = \frac{\left(1 + E_1\cos\alpha\right)\left(1 - E_1\right)}{1 - E_{1,\mathrm{app}}^2} M_0, \tag{4}$$

where M_0 is equilibrium magnetization.

Next, the longitudinal magnetization for flowing spin ($M_{\mathrm{ss},z}$) was estimated from the following equations:

$$M_{n,z} = E_{1,\mathrm{app2}}^{n}\left(M_{\mathrm{ini},z} - M_{\mathrm{ss},z}\right) + M_{\mathrm{ss},z}, \tag{5}$$

where $E_{1,\mathrm{app2}}$ is an apparent T_1 decay over two periods of DANTE pulses for flowing spin, which is estimated from the following equations:

$$E_1 = \mathrm{e}^{\left(-TR/T_{1,\mathrm{arteiral\ blood}}\right)}, \tag{6}$$

$$E_{1,\mathrm{app2}} = E_1 \cos\alpha. \tag{7}$$

The longitudinal magnetization for flowing spin ($M_{\mathrm{ss},z}$) was finally calculated using the following equation:

$$M_{\mathrm{ss},z} = \frac{\left(1 - E_1\right)}{1 - E_1\cos\alpha} M_0. \tag{8}$$

Details of the derivation of the formulas for the estimation of flowing spin are described elsewhere [14]; however, it should be noted that derivation of the equation which estimates the flowing spin assumes complete loss of coherence during the DANTE pulses.

Thereafter, the theoretical phase shift induced by the flow velocity in each experimental condition was calculated and compared with that used for the 3-dimensional gradient and spin echo (3D GRASE) sequence in a previous report [14]. Additionally, the phase shift from off-resonance in static spins was calculated.

Phantom study

The perfusion phantom, which consists of labeling, perfusion, and a pump section, was used (FUYO Corporation, Tokyo, Japan). Figure 2 shows the schematic of the perfusion phantom used in our study. The labeling section was made of silicon tubes with a diameter of 3.0 mm. The perfusion section was composed of three urethane densities with

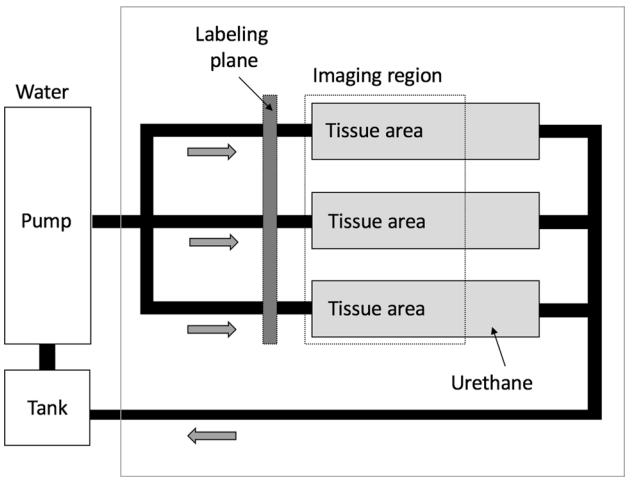

Fig. 2 Schematic of the perfusion phantom, which consists of labeling and imaging sections. There are tissue areas with different densities of urethane (0.80±0.16, 1.2±0.16, and 1.6±0.16 holes/mm). The arterial spin labeling images were acquired with three flow velocities in the tissue area. The flow velocities immediately after entering the tissue area were 2.0, 4.2, and 5.7 cm/s

different number of holes per length (0.80 ± 0.16, 1.2 ± 0.16, and 1.6 ± 0.16 holes/mm), to change the flow velocity of the perfusion section.

To evaluate the impact of the FA and GA of the DANTE, ASL images were obtained with three flow velocities and various parameters of the DANTE using the perfusion phantom. The flow settings for the perfusion phantom and parameters of the DANTE were as follows: flow velocity in the imaging area: 2.0, 4.2, and 5.7 cm/s; FA: 0°–15° at 5-degree intervals; GA: 0–20 μs T/m at 5 μs T/m intervals, respectively. The imaging parameters of the ASL were as follows: labeling duration, 4.0 s; post-labeling delay time, 700 ms; field-of-view, 240 × 240 mm^2; sampling points, 512; arms, 7; number of excitations, 1; receive bandwidth, 976.6 Hz/pixel; repetition time (TR), 6184 ms; echo time (TE), 10.5 ms; slice thickness, 4.0 mm; number of slices, 38 slices. The proton density weighted images without labeling and DANTE were acquired at the same imaging settings. The relative signal intensity was calculated by the dividing the signal intensity at each GA setting by that at a GA of 0 μs T/m; these were compared across all DANTE and flow velocity conditions.

In vivo study

Ten healthy volunteers (mean age 42.9 years; age range 23–56 years) were enrolled. All volunteers provided written informed consent. To assess the optimal DANTE parameters, ASL images of the volunteers were obtained with and without the DANTE under the same conditions as the phantom study.

The ΔM, which was the percent signal change between label and control in each tissue, in all imaging settings were calculated by dividing ASL images with proton density weighted images using MATLAB (MathWorks, Natick, MA). The ΔM with each DANTE condition was measured in each arterial territory, anterior cerebral artery (ACA), middle cerebral artery (MCA), and posterior cerebral artery (PCA), in all images of the volunteers. We selected images widely covering each arterial territory. The regions of interest were manually drawn on each image using ImageJ 1.50 (National Institutes of Health, Bethesda, MD). Since the relationship between FA and apparent T_1 value of moving spin was described by second order function [14], we assumed that the decrease for ΔM at larger FA could be fitted by a quadratic function. Since this reduction of ΔM should be directly associated with the flow velocity and the amount of microvascular signal, the coefficient of the quadratic term can be characteristic of the decrease in signal associated with the degree of the flowing spin. Therefore, mapping the quadratic term coefficient of the ΔM signal may reveal the relative microvascular signal. To assess the ratio of the ΔM decrease associated with increased FA at a GA of 10 μs T/m, the coefficient of quadratic term was calculated by the fitting of a quadratic function using ΔM with FAs of 0°, 5.0°, 7.5°, 10°, 12.5°, and 15°. The fitting was performed on a pixel-by-pixel basis for all image in all volunteers. Thereafter, we compared the average coefficient of quadratic term between the arterial territories on the map in all volunteers. Each region of interest of the arterial territory was the same as that drawn for the measurement of ΔM.

Statistical analysis

Statistical analysis was performed to identify significant differences between the coefficient of quadratic term of ΔM in each arterial territory using the Friedman test with post hoc Dunn's multiple comparison tests using the Prism 6.0 (GraphPad Software, Inc., La Jolla, CA). A p value < 0.05 was considered significant.

Results

Numerical simulation

Figure 3 shows the results of the numerical simulation, which was calculated under the assumption that the flowing spin completely lost its coherence. The results of numerical simulation revealed that the magnetization of flowing spins decreased with larger FA. The decrease in the magnetization plateaued at a FA of 12.5°. The magnetization of the static spins was constant at a FA of more than 5.0°. From both results, the contrast between the static spin and flowing spin was high and steady at FAs of more than 12.5°.

Table 1 demonstrates the number of bandings the moving spins go through in each condition based on the parameters of DANTE and on the flow velocities. Table 2 demonstrates the off-resonance effects of the static spins for each DANTE condition.

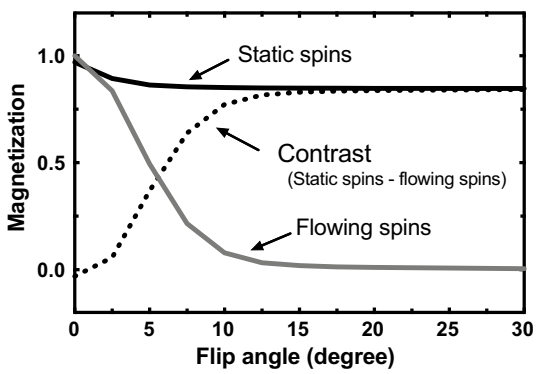

Fig. 3 The results of numerical simulation. The magnetization of moving spins decreased with larger flip angles (FAs). The decrease in the magnetization of moving spin was plateaued at a FA of 12.5°

Table 1 Additional phase shift due to the moving spin for each DANTE condition

	Gradient strength (mT/m)	Gradient duration (μs)	Grad area (μs T/m)	Time between RF pulses (ms)	Flow velocity (cm/s)	Number of RF pulses	Additional phase (radian)	Number of rotations	Flip angle (°)	Relative phase shift (%)	Relative suppression per total RF pulse (%)[a]
Our parameter	10	1000	10	1	0.5	200	4012.8	638	12.5	41.6	170
					1		8025.7	1277			
					5		40,128.3	6386			
					10		80,256.7	12,773			
					20		160,513.3	25,547			
Previous report [14]	6	2000	12	2	0.5	72	9630.8	1532	15	100	100
					1		19,261.6	3065			
					5		96,308.0	15,328			
					10		192,616.0	30,656			
					20		385,232.0	61,313			

[a]The suppression effect was calculated using Eq. (5) in the text ($T_1 = 1600$ms)

Phantom study

The phantom study showed that the ASL signals decreased with larger FAs for all the flow velocities, except in 5 μs T/m of GA at a flow velocity of 2.0 cm/s (Fig. 4). By increasing the setting of GA to 5–10 μs T/m, the difference in relative signal intensities corresponding to the flow velocity was increased. When GA was increased to ≥ 15 μs T/m, the difference in relative signal intensities corresponding to the flow velocity decreased. The relative signal intensity was observed to decrease with large values of FA for all settings of GA.

At fast flow velocities, the difference in ASL signals at each GA tended to decrease. However, with a flow velocity of 5.7 cm/s, the ASL signal with GA of 20 μs T/m decreased less than those with GAs of 10 and 15 μs T/m.

In vivo study

In the in vivo study, ΔM tended to decrease with large FA and GA in all arterial territories (Fig. 5), which was similar to the association of flow velocity with the FA of RF and GA of DANTE parameters, according to the results of the phantom study. However, particularly in the PCA region, when GA was > 15 μs T/m and FA > 12.5°, standard deviation of the ΔM increased (Fig. 5c). The representative in vivo ASL images obtained by applying the DANTE with various FAs at GA of 10 μs T/m are shown in Fig. 6. It was clearly observed that the ΔM was reduced with larger FAs. The coefficient of quadratic term of ΔM for each vascular region is shown in Fig. 7. The coefficient of quadratic term of the vascular regions of the MCA and ACA were significantly higher than that of the PCA ($p = 0.002$, and 0.022, respectively). Figure 8 shows the representative maps of the coefficient of quadratic term of ΔM for young and elderly adults (25 and 56 years old, respectively).

Discussion

The results of this study demonstrated that the DANTE at optimal conditions could effectively decrease the signal intensity in flowing spins that remained in the blood vessels.

The results of the numerical simulation showed that the theoretical signal intensities of static and flowing spins were constant when the FA was larger than 12.5°, and the suppression efficiency of the flowing signal had not changed despite increasing the FA further. These results are consistent with those of a previous study [14]. However, the numerical simulation did not consider the flow velocity; thus, we conducted a phantom experiment to investigate the dependency of flow

Table 2 The off-resonance phase shift of the static spin for each DANTE condition

	Gradient strength (mT/m)	Gradient duration (μs)	Grad area (μs T/m)	Time between RF pulses (ms)	Difference of Hz (Hz)	Number of rotations	Resolution (mm)
Our parameters	10	1000	10	1	0.0	0.0	0
					8025.7	8.0	1
					16,051.3	16.1	2
					24,077.0	24.1	3
					32,102.7	32.1	4
					40,128.3	40.1	5
					48,154.0	48.2	6
					56,179.7	56.2	7
	1	1000	1	1	0.0	0.0	0
	2		2		6420.5	6.4	4
	3		3		9630.8	9.6	4
	4		4		12,841.1	12.8	4
	5		5		16,051.3	16.1	4
	6		6		19,261.6	19.3	4
	7		7		22,471.9	22.5	4
Previous report [14]	6	2000	12	2	0.0	0.0	0
					4815.4	9.6	1
					9630.8	19.3	2
					14,446.2	28.9	3
					19,261.6	38.5	4
					24,077.0	48.2	5

velocity for suppressing the ASL signal, and to optimize the GA and the FA more thoroughly for applying DANTE to ASL imaging.

With regards to the application of the vascular suppression scheme in the perfusion of ASL, the primary DANTE parameters should be carefully considered. To strengthen the vascular suppression scheme, an increase in the number of RF and GA pairs or an increase in FA or gradient moment could be selected. Selection of the former pair may lead to an effective reduction of PLD, hence lowering the signal-to-noise ratio, whereas higher GA values may induce a comparatively larger eddy current effect, possibly leading to inhomogeneity of the perfusion signal [13]. If larger FA values are used, a stronger vascular suppression can be achieved but may result in a more T_1-weighted contrast of the perfusion image. Therefore, there is a tradeoff between these conditions on the extent of vascular suppression achieved.

We calculated the theoretical phase shift induced by flow velocity in each experimental condition and compared them to that used for the 3D GRASE sequence [14] (Table 1). By comparing the number of bandings in the calculated phase shift, we could predict the suppressive effect of flow spins since the flow spins traveling through these bandings may lead to the loss of their phase coherence. In addition, this may predict the extent of signal loss in the slow-moving spins in each DANTE condition. Moreover, due to the calculated off-resonance phase shift induced in each experimental DANTE condition, we could confirm that the selected setting could prevent the occurrence of banding artifacts for static spins (Table 2).

The results of the phantom study showed that an optimal setting of the DANTE could effectively decrease the spin signals under slow flow velocity conditions. The ASL signal intensity in the phantom decreased as the flow velocity increased. For larger FAs and GAs, the ASL signal intensity decreased further. Moreover, when the GA exceeded 15 μs T/m, the difference in relative signal intensities decreased depending on the flow velocity. Although the signal intensity showed a tendency to decrease with larger FA and GA values, the signal intensity obtained using the perfusion phantom did not reach a plateau despite using the largest value of FA. This is possibly due to the use of water instead of arterial blood as the flowing fluid (the T_1 value of water is more prolonged than that of arterial blood in vivo).

The in vivo study showed that larger GAs and FAs showed a tendency to decrease the relative signal intensity in all arterial territories. These results were similar to those of the phantom study. The relative signal intensities of all arterial territories were suppressed to 60% using a GA of 10 μs T/m and an FA of 12.5° for DANTE. Zhou et al. reported

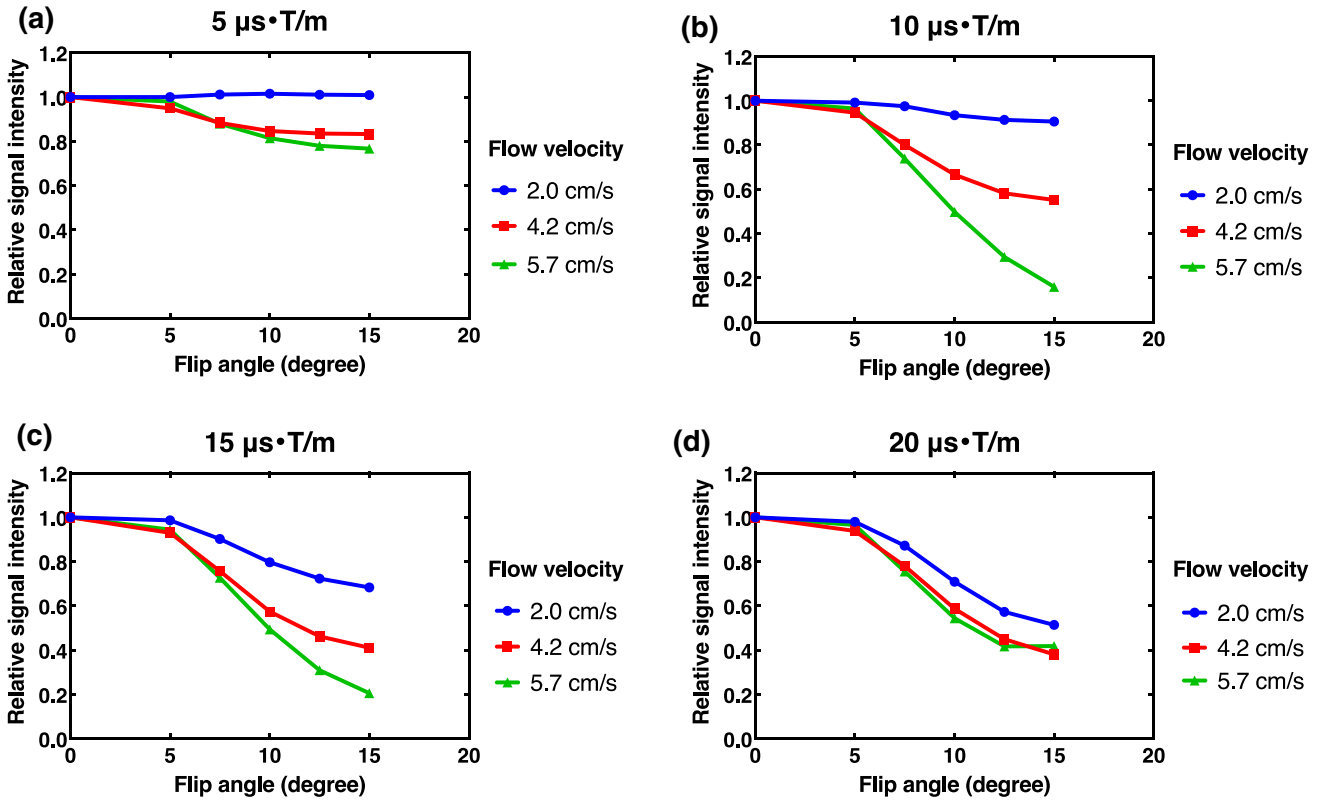

Fig. 4 The results of the phantom study. The relative signal intensities were decreased for a larger flow velocity. The flow velocity dependence decreased as the gradient area (GA) increased. For larger flip angles and GAs, the relative signal intensities were decreased

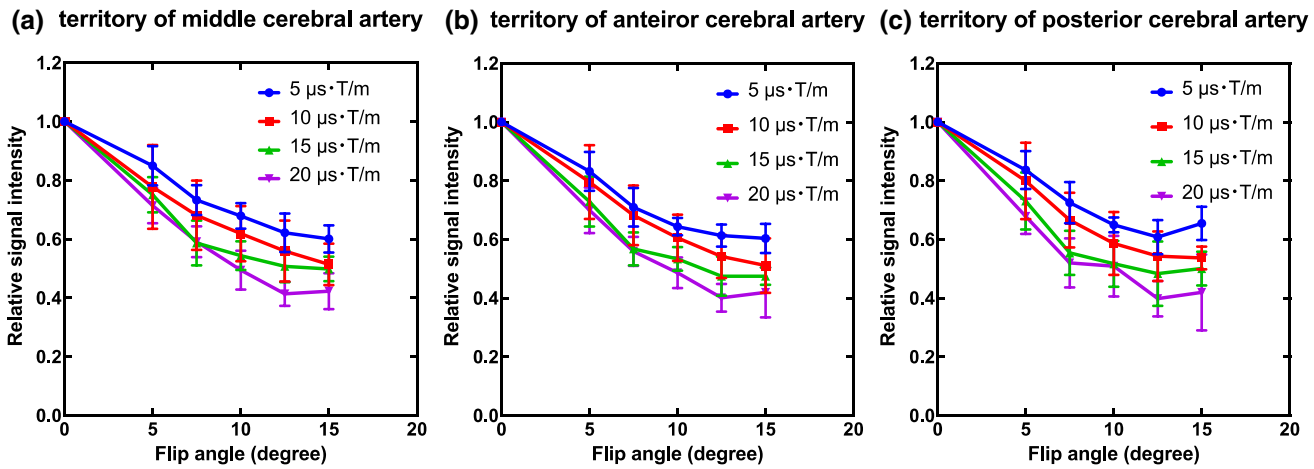

Fig. 5 The relationship between the relative signal intensity and flip angle (FA) for different gradient areas (GAs) in the middle, anterior, and posterior cerebral artery territories, respectively (**a**–**c**)

that the microvasculature signal comprised of approximately 40% of the ASL signal at the end label period. The ASL signal originating from static brain tissue made up 60% of all ASL signals [18]. The ΔM we obtained by applying DANTE under optimal conditions was consistent with their report.

Moreover, in all arterial territories, the relative signal intensity did not decrease linearly with an increase in FA at a GA more than 10 μs T/m for DANTE. For large values of FA and GA, although the value of ΔM was closer to the plateau due to the complete suppression of the moving spins

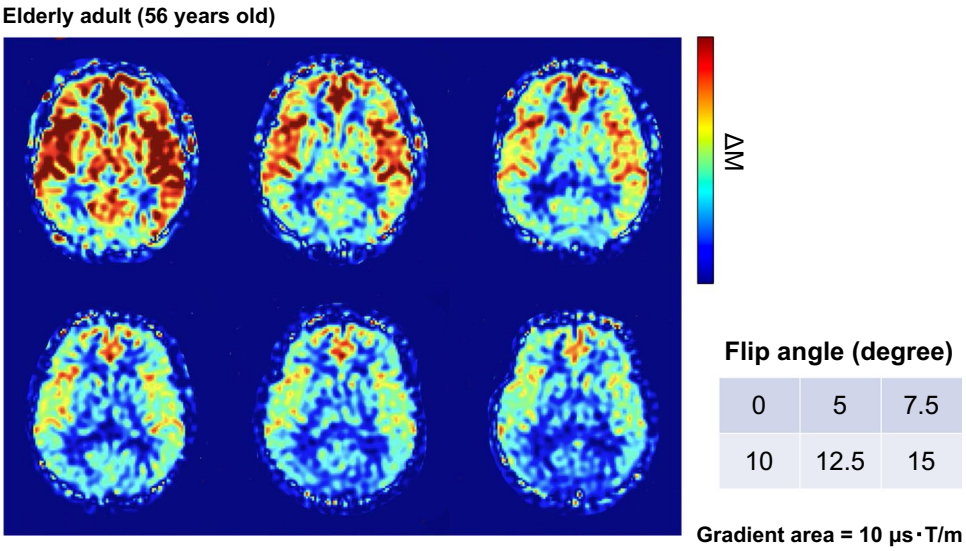

Fig. 6 Representative ΔM images in an elderly adult (56 years old) with different flip angles (FAs) and gradient area of 10 μs T/m. It is observed that the ΔM is decreased with larger FAs

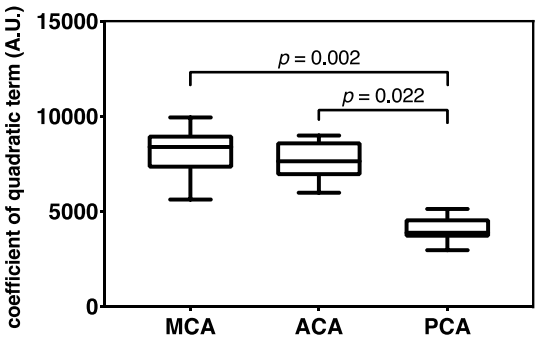

Fig. 7 The result of the coefficient of quadratic term calculated from ΔM with multiple flip angles. The coefficient of quadratic term of the ΔM in the posterior cerebral artery (PCA) territory was significantly smaller than those of the middle (MCA) and anterior cerebral artery (ACA) territories

by DANTE, the standard deviation had increased. This may be because the large values of GA and FA caused a decrease in the image uniformity or signal-to-noise ratio due to the inhomogeneity of B_1 and eddy currents [11, 12].

Therefore, to uniformly suppress the ASL signal from the arterial vascular spin, the use of a larger GA over 15 μs T/m should be avoided. From these results, we determined that the optimal conditions for FA and GA were 12.5° and 10 μs T/m, respectively. Therefore, it was considered that the optimized DANTE pulse aids in efficiently and uniformly suppressing the microvascular signal, depending on the flow velocity.

We assumed that high flow signals from macro- or microvascular regions could easily lead to a loss in coherence, and that relatively slower flow signals from the tissue compartment may be retained as perfusion signal even after the DANTE suppression scheme. Figure 6 showed that the loss of the large perfusion signal was apparent with an initial increase of FA in certain surface areas of the brain, such as the insular and frontal sulci, where relatively higher flow signals were expected. Moreover, the high value shown in Fig. 8 clearly corresponded with the anatomical macro-vascular path on the surface of the brain, since large coefficient values of the quadratic term revealed an early loss of signal with a corresponding increase of FA.

In the in vivo study, the coefficients of the quadratic term of ACA and MCA territories were significantly higher than that of PCA. Theoretically, the quadratic term coefficient calculated by multiple ASL images with different suppression strengths for blood vessel spins using DANTE should represent macrovascular spins at the location. This is because the decrease in ASL signal correlates with moving spins in the area. Therefore, our results indicate that the quadratic term coefficient of PCA was smaller than those of the MCA and PCA and indicates that macrovascular spins in the PCA territory was larger than that in other arterial territories. However, the coefficient of the quadratic term may be not always a significant value to represent the macrovascular signal due to the non-linear relationship between the FA values and relative signal intensity. It is well known that the flow velocity of the PCA is slower than that of the ACA and MCA [19]. Therefore, the labeled spins in the PCA macrovascular space may be larger than other regions. The significant differences in the coefficient of quadratic term between the PCA and other arterial territories in our study corresponded to those of previous reports [19, 20]. Therefore, the macrovascular signal map of labeled spins may be useful for assessing changes in the hemodynamic state.

Our study has several limitations. First, the sample size was small and included healthy volunteers. Second, the clinical effectiveness of the macrovascular signal map was not evaluated in this study. In the future, this evaluation will be needed for patients with cerebrovascular disease,

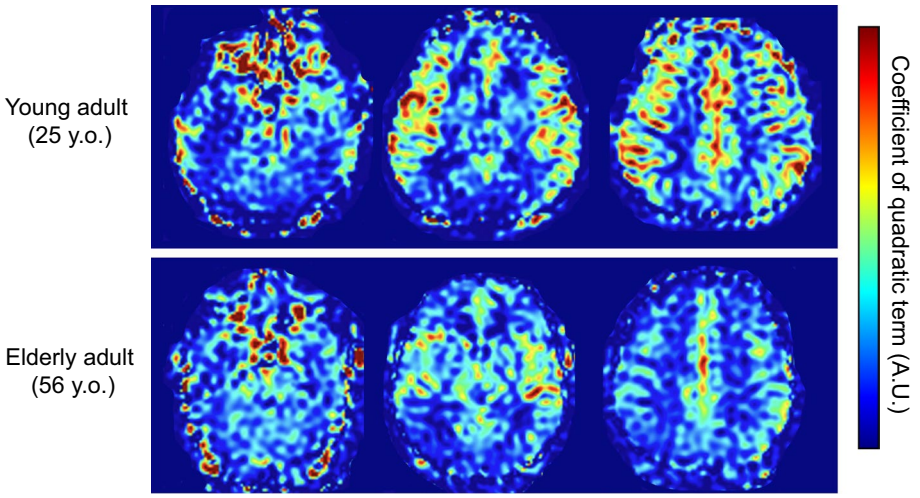

Fig. 8 Representative coefficient of quadratic term maps for young and elderly adults (25 and 56 years old, respectively) in each arterial territory for the in vivo study. Particularly, the coefficient of the quadratic term in the level of the anterior cerebral artery (ACA, such as shown in the right column) and middle cerebral artery (MCA, such as shown in the middle column) territories are different in each adult. These differences may indicate that labeled spins have different flow velocity characteristics depending on the region of the brain and on the subject. PCA: posterior cerebral artery

such as cerebral infarction, moyamoya disease, and internal carotid artery occlusion.

Third, the DANTE pulse was only applied in the direction of the static magnetic field (B_0). Theoretically, the movement of the labeled spins in different directions to the B_0 cannot be suppressed. However, majority of the labeled spins in blood vessels have a velocity component in the B_0 direction, which travels towards the top of the head when the DANTE pulse is applied. Therefore, we believed that applying the DANTE pulse only in the direction of B_0 is effective to suppress the vascular spins. If the DANTE pulse is applied along the other two orthogonal directions perpendicular to the B_0, a more suppressed vascular signal may be obtained; however, they may cause inhomogeneity in the DANTE pulse and prolong the imaging time. Therefore, the DANTE pulse was only applied along the direction of the B_0 as described in other reports [14].

Finally, the flow velocity of the phantom study at the perfusion section was set to 2–5 cm/s. This setting was larger than the DANTE's cutoff velocity of 2–3 mm/s. Since our phantom could not build a stable condition with an extremely slow flow, we could not measure or confirm the signal change in these conditions. In the future, more detail control of the extremely slow flow velocity would be needed to evaluate the dependency of the flow velocity.

In conclusion, an optimized DANTE makes it possible to efficiently suppress the macro-and micro-vascular signals depending on the flow velocity. Moreover, the macrovascular signal mapping of labeled spins may be useful to assess the altered hemodynamic state.

Acknowledgements This work was supported in part by the Grants-in-Aid for Scientific Research (C) 18K07670 from the Japan Society for the Promotion of Science.

Author contributions YF: study conception and design, acquisition of data, analysis and interpretation of data, drafting manuscript, critical revision. HK: study conception and design, critical revision. SI: study conception and design, acquisition of data, analysis and interpretation of data, critical revision. MK: study conception and design, acquisition of data, analysis and interpretation of data, critical revision. NT: study conception and design, acquisition of data, analysis and interpretation of data, critical revision. TM: study conception and design, acquisition of data, analysis and interpretation of data, critical revision. NK: analysis and interpretation of data, drafting manuscript, critical revision. TA: acquisition of data, analysis and interpretation of data, critical revision.

Compliance with ethical standards

Conflict of interest Naoyuki Takei is an employee of GE Healthcare Japan Corporation.

Ethical approval All procedures performed in studies involving human participants were in accordance with the ethical standards of the institutional and/or national research committee (institutional review board of the University of Fukui) and with the 1964 Helsinki declaration and its later amendments or comparable ethical standards. Informed consent was obtained from all individual participants for the in vivo study.

References

1. Williams DS, Detre JA, Leigh JS, Koretsky AP (1992) Magnetic resonance imaging of perfusion using spin inversion of arterial water. PNAS 89:212–216

2. Detre JA, Leigh JS, Williams DS, Koretsky AP (1992) Perfusion imaging. Magn Reson Med 23:37–45
3. Dai W, Garcia D, de Bazelaire C, Alsop DC (2008) Continuous flow-driven inversion for arterial spin labeling using pulsed radio frequency and gradient fields. Magn Reson Med 60:1488–1497
4. Chalela JA, Alsop DC, Gonzalez-Atavales JB, Maldjian JA, Kasner SE, Detre JA (2000) Magnetic resonance perfusion imaging in acute ischemic stroke using continuous arterial spin labeling. Stroke 31:680–687
5. Weber MA, Zoubaa S, Schlieter M, Jüttler E, Huttner HB, Geletneky K, Ittrich C, Lichy MP, Kroll A, Debus J, Giesel FL, Hartmann M, Essig M (2006) Diagnostic performance of spectroscopic and perfusion MRI for distinction of brain tumors. Neurology 66:1899–1906
6. Kimura H, Kado H, Koshimoto Y, Tsuchida T, Yonekura Y, Itoh H (2005) Multislice continuous arterial spin-labeled perfusion MRI in patients with chronic occlusive cerebrovascular disease: a correlative study with CO_2 PET validation. J Magn Reson Imaging 22:189–198
7. Ye FQ, Pekar JJ, Jezzard P, Duyn J, Frank JA, McLaughlin AC (1996) Perfusion imaging of the human brain at 1.5 T using a single-shot EPI spin tagging approach. Magn Reson Med 36:219–224
8. Amukotuwa SA, Yu C, Zaharchuk G (2015) 3D Pseudocontinuous arterial spin labeling in routine clinical practice: a review of clinically significant artifacts. J Magn Reson Imaging 43:11–27
9. Ferré J-C, Bannier E, Raoult H, Mineur G, Carsin-Nicol B, Gauvrit J-Y (2013) Arterial spin labeling (ASL) perfusion: techniques and clinical use. Diagn Interv Imaging 94:1211–1223
10. Watts JM, Whitlow CT, Maldjian JA (2013) Clinical applications of arterial spin labeling. NMR Biomed 26:892–900
11. Alsop DC, Detre JA, Golay X, Günther M, Hendrikse J, Hernandez-Garcia L, Lu H, MacIntosh BJ, Parkes LM, Smits M, van Osch MJP, Wang DJJ, Wong EC, Zaharchuk G (2014) Recommended implementation of arterial spin-labeled perfusion MRI for clinical applications: a consensus of the ISMRM perfusion study group and the European consortium for ASL in dementia. Magn Reson Med 73:102–116
12. Wang J, Yarnykh VL, Hatsukami T, Chu B, Balu N, Yuan C (2007) Improved suppression of plaque-mimicking artifacts in black-blood carotid atherosclerosis imaging using a multislice motion-sensitized driven-equilibrium (MSDE) turbo spin-echo (TSE) sequence. Magn Reson Med 58:973–981
13. Matsuda T, Kimura H, Kabasawa H, Kanamoto M (2018) Three-dimensional arterial spin labeling imaging with a DANTE preparation pulse. Magn Reson Imaging 49:131–137
14. Li L, Miller KL, Jezzard P (2012) DANTE-prepared pulse trains: a novel approach to motion-sensitized and motion-suppressed quantitative magnetic resonance imaging. Magn Reson Med 68:1423–1438
15. Bouvy WH, Geurts LJ, Kuijf HJ, Luijten PR, Kappelle LJ, Biessels GJ, Zwanenburg JJM (2016) Assessment of blood flow velocity and pulsatility in cerebral perforating arteries with 7-T quantitative flow MRI. NMR Biomed 29:1295–1304
16. Petersen ET, Lim T, Golay X (2006) Model-free arterial spin labeling quantification approach for perfusion MRI. Magn Reson Med 55:219–232
17. Kamano H, Yoshiura T, Hiwatashi A, Abe K, Togao O, Yamashita K, Honda H (2013) Arterial spin labeling in patients with chronic cerebral artery steno-occlusive disease: correlation with 15O-PET. Acta Radiol 54:99–106
18. Zhou J, Wilson DA, Ulatowski JA, Traystman RJ, van Zijl PC (2001) Two-compartment exchange model for perfusion quantification using arterial spin tagging. J Cereb Blood Flow Metab 21:440–455
19. Fujiwara Y, Matsuda T, Kanamoto M, Tsuchida T, Tsuji K, Kosaka N, Adachi T, Kimura H (2016) Comparison of long-labeled pseudo-continuous arterial spin labeling (ASL) features between young and elderly adults: special reference to parameter selection. Acta Radiol 58:84–90
20. Sorteberg W, Lindegaard KF, Rootwelt K, Dahl A, Russell D, Nyberg-Hansen R, Nornes H (1989) Blood velocity and regional blood flow in defined cerebral artery systems. Acta neurochir 97:47–52